Pattern Recognition Letters 30 (2009) 449–455

Contents lists available at ScienceDirect

Pattern Recognition Letters

journal homepage: www.elsevier.com/locate/patrec

Robust image corner detection based on scale evolution difference of planar curves

Xiaohong Zhang [a,*], Honxing Wang [b], Mingjian Hong [a], Ling Xu [a], Dan Yang [a], Brian C. Lovell [c]

[a] School of Software Engineering, Chongqing University, Chongqing 400030, PR China
[b] College of Mathematics and Physics, Chongqing University, Chongqing 400030, PR China
[c] School of Information Technology and Electrical Engineering, The University of Queensland, St. Lucia, Brisbane 4072, Australia

ARTICLE INFO

Article history:
Received 31 January 2008
Received in revised form 22 October 2008
Available online 17 November 2008

Communicated by H.H.S. Ip

Keywords:
Evolution difference
Evolution similarity
Corner detection
Difference of Gaussian
Planar curve

ABSTRACT

In this paper, a new corner detector is proposed based on evolution difference of scale pace, which can well reflect the change of the domination feature between the evolved curves. In Gaussian scale space we use Difference of Gaussian (DoG) to represent these scale evolution differences of planar curves and the response function of the corners is defined as the norm of DoG characterizing the scale evolution differences. The proposed DoG detector not only employs both the low scale and the high one for detecting the candidate corners but also assures the lowest computational complexity among the existing boundary-based detectors. Finally, based on ACU and Error Index criteria the comprehensive performance evaluation of the proposed detector is performed and the results demonstrate that the present detector allows very strong response for corner position and possesses a better detection and localization performance and robustness against noise.

1. Introduction

Corners in images represent much useful information and they play an important role in describing object features for recognition and identification. Applications that rely on corners include scene analysis, stereo matching, robot navigation, stitching of panoramic photographs and object tracking, among many others. For this reason, considerable work has been performed on corner detection and many algorithms for detecting the corners have been developed in recent years. These algorithms may be divided into two main groups. The first group contains the algorithms that work directly with the values of brightness of images (without segmenting the image in advance), such as Moravec et al. (1977), Harris et al. (1987), Dreschler and Nagel (1981), Kitchen and Rosenfeld (1982), Fang and Huang (1982), Smith and Brady (1994), Chen et al. (1995), Cheol Bae et al. (2002) etc. detectors. The other group includes the algorithms that extract the boundary first and analyze its shape afterwards. The algorithm we propose falls into this category. In the following, we will briefly describe the main approaches that appeared in the history of boundary-based detectors.

Among all boundary-based detectors Curvature Scale Space (CSS) is one of the most efficient techniques for corner detection and has been used in several corner detectors (Rattarangsi and Chin, 1992; Mokhtarian and Suomela, 1998; Mokhtarian and Suomela, 2001; Mohanna and Mokhtarian, 2001; He and Yung, 2004; Zhang et al., 2007). The main reason is that CSS has very good evolution similarity for the evolved planar curves. For example, as the scale is increased, the noise is smoothed away and the effect of the noise on the domination feature such as the curvature is reduced. However, as the contour evolves, the actual locations of the domination points change. Tracking from high to low scale is necessary to assure that the corner detection is not affected by the noise and the localization of the corners is good. But, this not only increases computing load but also results in other problems. For instance, as the contour evolves, some weak domination points may disappear so that there is difficulty in choosing an appropriate scale for assuring the true corners can be detected. On the other hand, in CSS methods the high order derivative, which is sensitive to the noise, is required for calculating curvature. In order to avoid choosing an appropriate scale due to the single scale detection, Zhang et al. (2007) suggested a scale product function defined as the multiplication of the curvatures of the contour at scales in framework of CSS, and corners were constructed as the local maxima beyond threshold. Although multiscale product can combine several scale information for localizing the corners it also increases computing load. Another popular method is based on wavelet transform of contour orientation (Lee et al., 1995; Quddus and Gabbouj, 2002; Gao et al., 2007) or eigenvectors (Yeh, 2003) of covariance matrices that denote tangent orientation of the planar curves, but there exists some drawbacks such as high false alarm rate besides the difficulty in choosing a proper scale. In fact, since their wavelet functions are chosen as B-Spline ones wavelet transform of contour orientation is essentially equivalent to the second order derivative

* Corresponding author. Tel.: +86 23 60606391; fax: +86 23 65111025.
E-mail address: xhongz@yahoo.com.cn (X. Zhang).

0167-8655/$ - see front matter © 2008 Elsevier B.V. All rights reserved.
doi:10.1016/j.patrec.2008.11.002

of the smoothed curves (Lee et al., 1995; Quddus and Gabbouj, 2002; Gao et al., 2007; Yeh, 2003), which is very sensitive to the noise. In Tsai et al. (1999) suggested a good measure for corner response by using the eigenvalues of the covariance Matrices of boundary coordinate points over a small region of support due to the fact that the smaller eigenvalue of covariance matrix reflected shape information of contour and the eigenvalues of the matrix could be used to extract the shape information. Its localization is good and the derivative of planar curves is not required, but it is very difficult to determine an appropriate width of support of region (ROS) for different type images while time complexity of eigenvalues is high. The major reason is that the smaller ROS is, the more sensitive to noise the detector is; the larger ROS is, the higher false alarm or missed rate the adjacent corners results in. Besides the typical boundary-based corner detectors discussed the others are referred to reference reviews of literatures (Tsai, 1997; Masood and Sarfraz, in press; Sobania and Evans, 2005; Arrebola and Sandoval, 2005; Guru and Dinesh, 2004). Based on the previous discussion we have found that the existing boundary-based detectors had considered the evolution similarities of scale space, thus the only single scale used for detecting candidate corners is inevitable and the proper one is difficultly determined.

On the contrary, little attention has been paid to the Evolution Difference between the evolved planar curves. In this paper, we have found that among the evolved planar curves there is another feature, which is referred to as *evolution difference* between the evolved versions. That is, the changes of the evolved curves have distinctive difference between corner positions and non-corner positions. The change in neighborhood of corner points is sharp whereas the change in neighborhood of non-corner positions is weak. Hence, we will employ these intrinsic evolution differences for presenting a new corner detection method, which utilizes both the low scale and the high one for determining the candidate corners. The contributions of this paper are as follows:

- We illustrate the motivation of the proposed algorithm by analyzing the evolution similarities and the evolution differences among the evolved curves based on scale space technique. Moreover, the evolution differences are viewed as the basic idea of our algorithm (Section 2.1).
- Based on Gaussian scale space we utilize Difference of Gaussian to reflect the evolution difference, which may be characterized by the norm of DoG. Naturally, the norm of DoG is defined as response function of corner detection (Section 2.2).
- In order to analyze the corner detection and localization performance of DoG, we discuss the relationship between the extreme points of DoG's norm and the curvature, and then conclude that the maxima of the DoG's norm correspond to ones of the curvature. Furthermore, we discuss the advantages of DoG over the curvature (Section 2.3).
- Finally, we carry out a comprehensive evaluation to study on the detection and localization performances of the detectors. The DoG corner detector outperformed the CSS and wavelet and covariance matrix detectors according to ACU He and Yung, 2004 and Error Index Lowe, 2004 criteria (Section 3).

2. Corner detection algorithm based on DoG

2.1. Motivation

Let $C(u)$ represent a regular planar curve as following:

$$C(u) = (x(u), y(u)) \tag{1}$$

where u is the any parameter, and $x(u)$ and $y(u)$ denote coordinate functions of planar curve, respectively.

The planar curve is first smoothed by convolution with Gaussian function

$$G(u,\sigma) = \frac{1}{\sqrt{2\pi\sigma^2}} \exp(-u^2/2\sigma^2)$$

where σ is standard deviation.

We have

$$\begin{aligned} C(u,\sigma) &= G(u,\sigma)^* C(u) = (G(u,\sigma)^* x(u), G(u,\sigma)^* y(u)) \\ &= (X(u,\sigma), Y(u,\sigma)) \end{aligned} \tag{2}$$

where * denotes convolution operator.

As shown in Fig. 1b–f, a leaf curve evolves at different scales according to (2). In the evolution process of the leaf, there are the following similarities among the evolved versions. As the scale increases, the noise is smooth away and the sharp corners remain whereas the weak corners will trend to disappear and the actual locations of the corners change. All existing curvature scale space (CSS) detectors use these similarity features through calculating the curvature of the evolved versions. But these detectors only consider a single scale in the candidate corner detection and the locations of the corners are updated by the coarse-to-fine tracking.

It is important to point out that besides the evolution similarities of scale space there is another distinctive evolution feature, which is referred to as *evolution difference* between the lower evolution version and the higher one. For example, Fig. 2a illustrates the two evolved curves of the leaf at the scales 2 and 5. We can observe that there are the obvious evolution differences between the neighborhoods of the corners of the two evolved curves. Moreover, the nearer the position far from a corner is, the more distinctive the evolution difference is. Fig. 2b–d, respectively, shows the evolved curves of the leaf between the scale 2 and another high scale, such as 10, 15 and 20. From those figures we can also observe that though the evolution differences are also observable at the non-corner positions there exist the maximal evolution differences at the corners. Moreover, as the scale increases, the maximal properties of the evolution differences at the corners are still preserved and the positions corresponding to the maximal evolution differences are not only affected by the high scale. Naturally, we can make use of the *evolution difference* of two evolved curves, where one scale is low enough to ensure good localization, the other is high enough to ensure the good anti-noise performance. So, we think that the evolution difference can better reflect the domination feature of the planar curves than the evolution similarities.

Now, how do we measure these evolution differences? Can the measurement of the evolution differences be used for the cornerness? If possible, what advantages has the new cornerness? In this paper, we will utilize Gaussian scale space to answer the above problems. And then we can construct a new corner detection algorithm by the measure of the evolution differences. This is the main idea of our paper.

Remark 1. It is important to point that in other scale space there also is the same scale evolution difference.

2.2. DoG operator for planar curves

In this section, we will directly give the definition for *Difference of Gaussian* of planar curves to measure the evolution differences. By (2), the second smoothed planar curve with a different standard deviation $m\sigma$ can be obtained:

$$\begin{aligned} C(u,m\sigma) &= G(u,m\sigma)^* C(u) = (G(u,m\sigma)^* x(u), G(u,m\sigma)^* y(u)) \\ &= (X(u,m\sigma), Y(u,m\sigma)) \end{aligned} \tag{3}$$

where $m\sigma = m \times \sigma$, "$\times$" denotes ordinary multiplication, i.e., $m > 1$ is a multiplier factor.

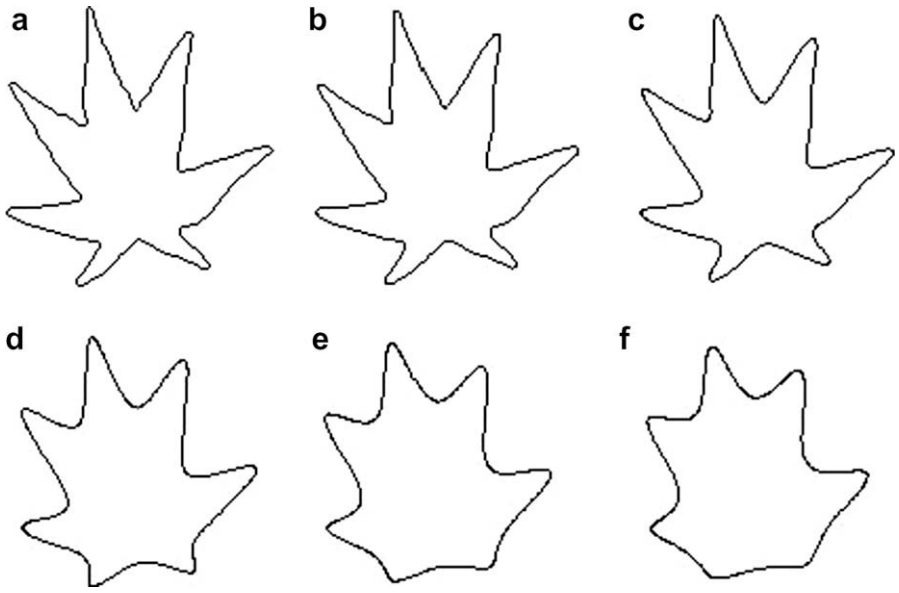

Fig. 1. Leaf and its evolved versions: (a) original; (b) $\sigma = 2$; (c) $\sigma = 5$; (d) $\sigma = 10$; (e) $\sigma = 15$; (f) $\sigma = 20$.

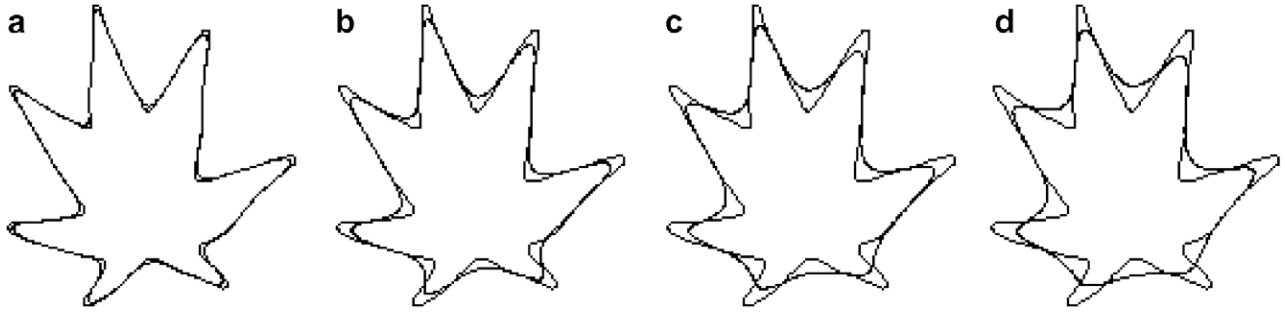

Fig. 2. Evolution difference between the two evolved versions, (a) $\sigma = 2$ and $\sigma = 5$; (b) $\sigma = 2$ and $\sigma = 10$; (c) $\sigma = 2$ and $\sigma = 15$; (d) $\sigma = 2$ and $\sigma = 20$.

Eqs. (2) and (3), respectively, express the two evolved curves at difference scales. According to the intuitive observation for Fig. 2, the evolution differences may be represented by the distance between the corresponding points of the two evolved curves. Thus, we define evolution difference as the following distance

$$\begin{aligned} D(u,\sigma) &= [G(u,m\sigma)^* x(u) - G(u,\sigma)^* x(u)]^2 \\ &\quad + [G(u,m\sigma)^* y(u) - G(u,\sigma)^* y(u)]^2 \\ &= [(G(u,m\sigma) - G(u,\sigma))^* x(u)]^2 + [(G(u,m\sigma) \\ &\quad - G(u,\sigma))^* y(u)]^2 = [DoG^* x(u)]^2 + [DoG^* y(u)]^2 \end{aligned} \tag{4}$$

where

$$\begin{aligned} DoG &= G(u,m\sigma) - G(u,\sigma) \\ &= \frac{1}{\sqrt{2\pi}\sigma}\left[\frac{1}{m}\exp(-u^2/2m^2\sigma^2) - \exp(-u^2/2\sigma^2)\right] \end{aligned} \tag{5}$$

Remark 2. Eq. (4) obviously reflects the size of the evolution difference for the evolved curves, so it can be viewed as cornerness response function. According to the observation for the feature of the evolution difference, the corner is naturally defined as the local maximum of (4). Later, we will give the theoretical analysis for the proposed detector. So, based on (4) we obtain a new detector referred to as DoG detector.

Remark 3. In Eq. (4) the low scale and the high one of planar curves are contained, and then several scales are combined into detecting the candidate corners. Moreover, in (4) location of corner is affected by small scale, thus we can avoid tracking from high to low scale. Hence, the problem of the corner location changing at large scale may be overcome in certain degree. This result will be further discussed in subsection 2.3. Eq. (5) defines *Difference of Gaussian (DoG)*. By (3) and (5), we can define the difference of two Gaussian smoothed planar curves as

$$\begin{aligned} G(u,m\sigma)^* C(u) - G(u,\sigma)^* C(u) &= (G(u,m\sigma) - G(u,\sigma))^* C(u) \\ &= DoG^* C(u) \\ &= (DoG^* x(u), DoG^* y(u)) \end{aligned} \tag{6}$$

Obviously, (6) may also reflect evolution difference in the form of vector and (4) is viewed as norm of (6).

Remark 4. It is obvious that once DoG operator in (5) is pre-computed analytically, the proposed DoG detector will be of the lowest computational complexity among the existing corner detectors based on the boundary.

Remark 5. To calculate DoG operator, the discrete convolution kernel for DoG can be obtained by approximating the continuous expression of DoG given above. Again, it is necessary for the sum or average of all elements of the kernel matrix to be zero.

2.3. Corner detection and localization performance of DoG

In this section, we will analyze the detection and localization performance of DoG detector through discussing the relationship with DoG and the curvature, so as to answer why (4) is known as the cornerness and which advantages DoG detector has.

Let F represent the functions $X(u,\sigma)$, $Y(u,\sigma)$, $G(u,\sigma)$, $D(u,\sigma)$, $\kappa(u,\sigma)$, $x(u)$ or $y(u)$. Then $\dot{F}$, $\ddot{F}$ and $\dddot{F}$ are the first order derivative, the second order derivative, and the third order derivative of F with respect to u, respectively.

Firstly, we recall several formulas with respect to the curvature and the diffusion equation. According to Rattarangsi and Chin (1992) and Mokhtarian and Mackworth (1992), through redefining parameter u the curvature κ of a smoothed planar curve defined by (2) can be simplified as

$$\kappa(u,\sigma) = \dot{X}(u,\sigma)\ddot{Y}(u,\sigma) - \ddot{X}(u,\sigma)\dot{Y}(u,\sigma) \tag{7}$$

$$\text{such as } \dot{X}^2(u,\sigma) + \dot{Y}^2(u,\sigma) = 1 \tag{8}$$

where

$$\dot{X}(u,\sigma) = x(u)^*\dot{G}(u,\sigma), \ddot{X}(u,\sigma) = x(u)^*\ddot{G}(u,\sigma)$$
$$\dot{Y}(u,\sigma) = y(u)^*\dot{G}(u,\sigma), \quad \ddot{Y}(u,\sigma) = y(u)^*\ddot{G}(u,\sigma)$$

On the other hand, according to Lowe (2004) Gaussian function satisfies the following diffusion equation

$$\sigma\nabla^2 G(u,\sigma) = \frac{\partial}{\partial\sigma}G(u,\sigma)$$

where $\nabla^2 G(u,\sigma) = \ddot{G}(u,\sigma)$.

In addition, we know

$$\frac{\partial}{\partial\sigma}G(u,\sigma) \approx \frac{G(u,m\sigma) - G(u,\sigma)}{m\sigma - \sigma} = \frac{G(u,m\sigma) - G(u,\sigma)}{(m-1)\sigma}$$

Therefore, we have

$$G(u,m\sigma) - G(u,\sigma) \approx (m-1)\sigma^2\nabla^2 G(u,\sigma) = (m-1)\sigma^2\ddot{G}(u,\sigma) \tag{9}$$

By (4) and (9), we rewrite (4) as

$$\begin{aligned} D(u,\sigma) &= [x(u)^*(G(u,m\sigma) - G(u,\sigma))]^2 + [y(u)^*(G(u,m\sigma) - G(u,\sigma))]^2 \\ &\approx [x(u)^*(m-1)\sigma^2\nabla^2 G(u,\sigma)]^2 + [y(u)^*(m-1)\sigma^2\nabla^2 G(u,\sigma)]^2 \\ &= (m-1)^2\sigma^4\{[x(u)^*\ddot{G}(u,\sigma)]^2 + [y(u)^*\ddot{G}(u,\sigma)]^2\} \\ &= (m-1)^2\sigma^4[\ddot{X}^2(u,\sigma) + \ddot{Y}^2(u,\sigma)] \end{aligned} \tag{10}$$

In the following, based on Eqs. (7)–(10) we will discuss relationship between DoG and the curvature of planar curves. Now, let u satisfy $\dot{\kappa}(u,\sigma) = 0$, i.e., u is an extreme point of κ. So, from (7) we have

$$\dot{X}(u,\sigma)\dddot{Y}(u,\sigma) - \dddot{X}(u,\sigma)\dot{Y}(u,\sigma) = 0$$

where $\dddot{X}(u,\sigma) = \dot{x}(u)^*\ddot{G}(u,\sigma)$, $\dddot{Y}(u,\sigma) = \dot{y}(u)^*\ddot{G}(u,\sigma)$.

Further, we have

$$\dddot{X}(u,\sigma) = \frac{\dot{X}(u,\sigma)\ddot{Y}(u,\sigma)}{\dot{Y}(u,\sigma)} \tag{11}$$

By (11) and (10), we have

$$\begin{aligned} \dot{D}(u,\sigma) &= (m-1)^2\sigma^4[2\ddot{X}(u,\sigma)\dddot{X}(u,\sigma) + 2\ddot{Y}(u,\sigma)\dddot{Y}(u,\sigma)] \\ &= 2(m-1)^2\sigma^4\left[\frac{\ddot{X}(u,\sigma)\dot{X}(u,\sigma)\dddot{Y}(u,\sigma)}{\dot{Y}(u,\sigma)} + \ddot{Y}(u,\sigma)\dddot{Y}(u,\sigma)\right] \\ &= \frac{2(m-1)^2\sigma^4\dddot{Y}(u,\sigma)[\dot{X}(u,\sigma)\ddot{X}(u,\sigma) + \dot{Y}(u,\sigma)\ddot{Y}(u,\sigma)]}{\dot{Y}(u,\sigma)} \end{aligned}$$

Also, with respect to u calculating the derivative in the two sides of (8), we have

$$\dot{X}(u,\sigma)\ddot{X}(u,\sigma) + \dot{Y}(u,\sigma)\ddot{Y}(u,\sigma) = 0 \tag{12}$$

This implies

$$\dot{D}(u,\sigma) = 0$$

From this equation it follows that the extreme points of κ are yet the ones of D.

On the other hand, let u satisfy $\dot{D}(u,\sigma) = 0$, i.e., u is an extreme point of D. By (10) this implies

$$\ddot{X}(u,\sigma)\dddot{X}(u,\sigma) + \ddot{Y}(u,\sigma)\dddot{Y}(u,\sigma) = 0 \tag{13}$$

Hence, by (7) and (13) we have

$$\begin{aligned} \dot{\kappa}(u,\sigma) &= \dot{X}(u,\sigma)\dddot{Y}(u,\sigma) - \dddot{X}(u,\sigma)\dot{Y}(u,\sigma) \\ &= \dot{X}(u,\sigma)\dddot{Y}(u,\sigma) + \frac{\ddot{Y}(u,\sigma)\dddot{Y}(u,\sigma)}{\ddot{X}(u,\sigma)}\dot{Y}(u,\sigma) \\ &= \frac{\dddot{Y}(u,\sigma)[\dot{X}(u,\sigma)\ddot{X}(u,\sigma) + \dot{Y}(u,\sigma)\ddot{Y}(u,\sigma)]}{\ddot{X}(u,\sigma)} \end{aligned}$$

In same way as (12) calculating the derivative in the two sides of (8) with respect to u, it follows that

$$\dot{\kappa}(u,\sigma) = 0$$

This implies that the extreme points of D are yet the ones of κ.

In term of the above discussion, we draw the conclusions as follows:

- The extreme points of the DoG's norm correspond to the ones of the curvature of planar curvature. Therefore, DoG has not only the same good detection performance as the CSS-based detectors but also the lowest computational complexity.
- According to (10), the extreme of the DoG's norm is associated with low sigma σ, and then Localization of DoG is affected by low sigma of DoG and not affected by high sigma of DoG. Therefore, DoG detector does not require tracking from high to low scale to improve corner locations and overcome the difficulty in choosing the high scale.

Remark 6. If DoG operator is directly performed according to (4), *DoG* operator has two important parameters σ and m. In our experiments, m is chosen as 1.5, and σ generally is chosen as some value in interval Harris et al., 1987. It is important to remember that value of σ is decided by image noise level.

Remark 7. There are local maxima of the DoG's norm on the evolved contours due to rounded corners or noise. These can be removed by introducing a threshold value t. Hence, the true corners commonly correspond to the local extrema of DoG that exceed the given global threshold. Global threshold size is affected by σ and m. Generally, threshold increases as σ increases. For example, when σ is chosen as 2, the threshold is set as 0.05; when σ is chosen as 2.5, the threshold is set as 0.1.

3. Performance evaluation and experimentations

In this section, we will compare the proposed DoG detector with Harris et al. (1987) and several typical boundary-based corner detectors including CSS (Mokhtarian and Suomela, 1998), eigenvalues of covariance matrices (Tsai et al., 1999), wavelet transform

(Lee et al., 1995), and eigenvectors of covariance matrices (Yeh, 2003) by using two criteria – accuracy (ACU) (Mohanna and Mokhtarian, 2001) and Error Index (Sojka, 2002). For convenience, we simplify these detectors as DoG, Harris, CSS, Eigenvalue, Wavelet and Eigenvector.

3.1. Image database

To conduct plenty of experiments we used the twenty different original images, which included Block, House, Lab, Pentagon, Airplane, Flower, Leaf, Gear, Key, Fish, Shark, and simple planar curves, etc. These images were used for the experiments in (Rattarangsi and Chin, 1992; Mokhtarian and Suomela, 1998; Mokhtarian and Suomela, 2001; Mohanna and Mokhtarian, 2001; Zhang et al., 2007; Chen et al., 1995; Lee et al., 1995; Quddus and Gabbouj, 2002; Gao et al., 2007; Tsai et al., 1999; Yeh, 2003). We had their transformed images as test images, which were obtained by applying the five different types of experiments on each original image as follows:

Experiment 1. Rotation. In this experiment, the rotation transformation was performed. Firstly, the number and the position of corners were extracted in the original image. Secondly, the original image was rotated with rotation angle chosen by uniform steps of the interval $[-80°,+80°]$. Distance between consecutive steps was 10°. Finally, the number and the positions of corners in each rotated image were extracted.

Experiment 2. Uniform. In this experiment, the uniform transformation was carried out. We did the same for the original image and uniform scaling of this image with scale factors chosen by uniform sampling of the interval [0.5, 1.5]. Distance between consecutive samples was 0.1.

Experiment 3. Non-uniform. In this experiment we repeated the process of Experiment 2 for non-uniform scaling. The x-scale and y-scale parameters were chosen by uniform sampling of the intervals [0.5, 1.5], respectively.

Experiment 4. Affine transform. Affine transform is applied to the original image. Here we applied a rotation angle of $-10°$ and $+10°$ and combined with non-uniform scaling with the x-scale and y-scale parameters chosen by uniform sampling of the intervals [0.5,1.5], respectively. Distance between consecutive samples was 0.1.

Experiment 5. Noise. In this experiment Gaussian white noise was added to the original image with zero-mean and variances chosen by uniform sampling of the intervals [0.005, 0.05], respectively. Distance between consecutive samples was 0.005.

Therefore, all of the original images and their rotated, uniformly and non-uniformly scaled, affine transformed and noise disturbed images made up our image database together.

3.2. Evaluation criteria

To evaluate the robustness of the proposed algorithm under the rotation, scaling, affine transforms and noise disturbing, we introduce accuracy (ACU) (Mohanna and Mokhtarian, 2001) and Error Index (Sojka, 2002) criteria for measuring the localization accuracy and stability of corner detectors, respectively.

Mohanna and Mokhtarian (2001) presented the criterion of accuracy, which took account of the number of corners in original image as well as the number of corners in each of the transformed images. Let N_o be the number of the corners detected in the original image (note that $N_o \neq 0$), N_a the number of the corners matched in the original image when compared to the ground-truth corners and N_g the number of the corners in the ground-truth. The criterion of accuracy is

$$\mathrm{ACU} = N_a/N_o + N_a/N_g)/2 \times 100\%$$

where ACU stands for "accuracy".

On the other hand, as described in (Sojka, 2002), we have also evaluated the number of corners detected correctly, the number of corners that were missed, and the number of false detections. By a false detection it means the situation when a corner is detected at a point at which (near which) no real corner exists. The total error of the detector is defined to be the sum of the number of missed corners and false detections. Hence, Error Index is the ratio of total error to number of corners in the image.

Remark 8. We use ACU to describe the accuracy of corner detectors. The value of ACU for stable and accurate corner detectors should be close to 100%. The ground-truth is created by human judgment.

Remark 9. In the tests, Error Index is used to describe the error rate of corner detectors. The value of Error Index for stable and accuracy corner detectors should be close to zero. Also the reference solutions of ground-truth corners were prepared for the tests.

3.3. Experimental results

According to ACU and Error Index criteria the comparative experiments were carried out for Harris, DoG, CSS, Wavelet, Eigenvalue, and Eigenvector under rotation, scaling, affine transforms and noise disturbing. All experiments were based on the environment platform of ***Window*** *s-XP* 2.6GHz and ***Matlab***-7.0. Moreover, the parameters of each detector in all experiments were set as the

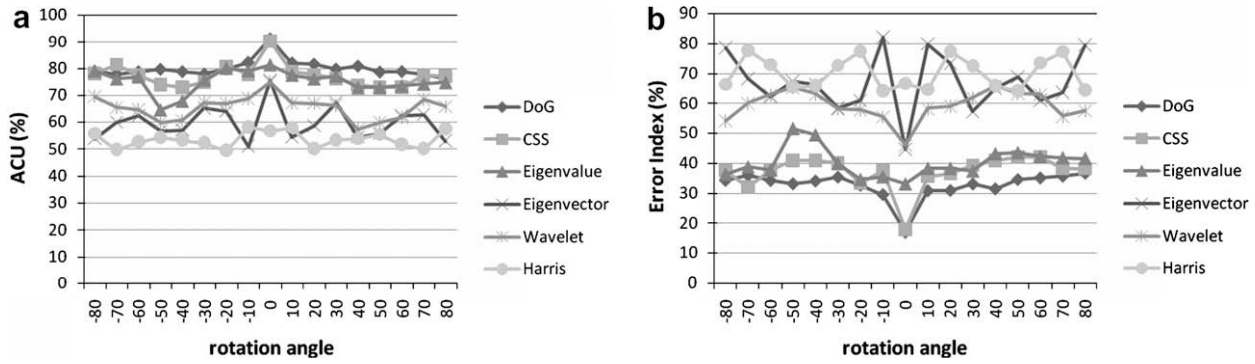

Fig. 3. ACU and Error Index under rotation: (a) ACU. (b) Error Index.

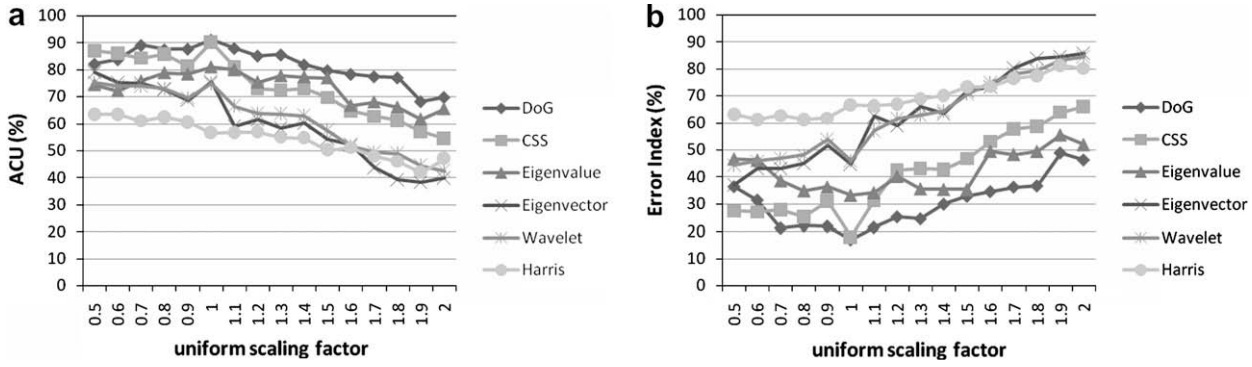

Fig. 4. ACU and Error Index under uniform scaling: (a) ACU. (b) Error Index.

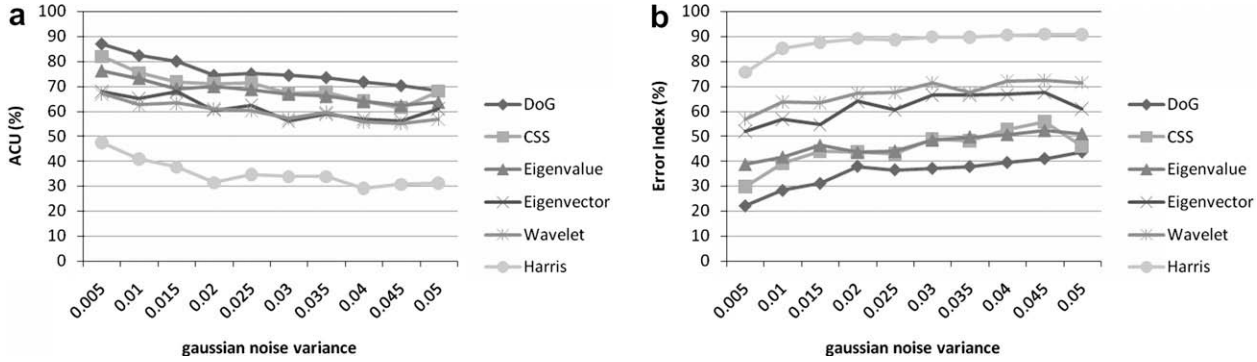

Fig. 5. ACU and Error Index values under noise disturbing: (a) ACU. (b) Error Index.

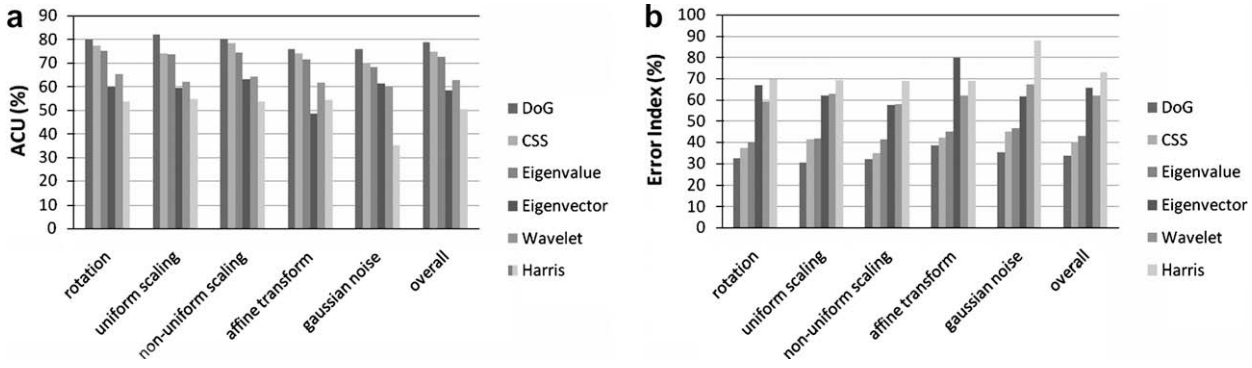

Fig. 6. The overall performance under various geometric transformations and the noise disturbing: (a) ACU. (b) Error Index.

values, which made each detector achieve as good as possible results for the images without any geometric transformation or noise disturbing and keep unchanged.

Figs. 3–5 illustrate the average values of ACU and Error Index under rotation, uniform scaling and noise disturbing, respectively. Note that these values are averaged across the all different images. Fig. 6 demonstrates the overall averages for ACU and Error Index under various transformations and Gaussian noise. And these results indicate the robustness of each detector under rotation, scaling and noise disturbing. As shown in Figs. 3–6, it follows that DoG offered the higher accuracy and the lower Error Index than the other five corner detectors under the various geometric transformations and the noise disturbing. On the other hand, from Fig. 6 we can also know overall ACU of DoG was up to above 75% under each transform and Error Index is less than 35%, moreover, they achieve the highest average values among the tested corners. All these results show that the detection performance of the DoG was better than the others, especially in the noise experiment (Fig. 5). In conclusion, all the evaluation results have shown that DoG had the best stability and accuracy with respect to similarity, affine transforms and noise disturbing.

4. Conclusions

In this paper, we first focused on the evolution similarities and the evolution differences of planar curves and found that the evolution difference can better reflect the domination structure feature of the planar curves than the evolution similarities. In the following, based on Gaussian scale space we defined a new

operator, i.e. DoG (Difference of Gaussian) operator of planar curves, whose norm represents and characterizes the evolution difference. Furthermore, it has been verified that the maxima of D*oG's Norm* corresponded to the ones of the curvature. Hence, we defined the norm of DoG as the response function. As a result, the main advantages of DoG lie in that DoG combines a low and a high scale into the detection of the candidate corner and the coarse-to-fine tracking may be avoided. Moreover, DoG has the lowest computing load among the existing boundary-based detectors. Finally, by using ACU and Error Index criteria we performed the comprehensive performance evaluation of the proposed detector. The experiments illustrated that the proposed DoG detector has generated good detection and localization under various geometrical transform and noise disturbing.

Acknowledgements

This work was supported by Notional Science Foundation (Grand No. 60604007), China, and Chongqing Science Foundation (Grand No. CSTC2005BA2002).

References

Arrebola, F., Sandoval, F., 2005. Corner detection and curve segmentation by multiresolution chain-code linking. Pattern Recognition 38 (10), 1596–1614.

Bae, S.C., Kweon, I.S., Yoo, C.D., 2002. COP: A new corner detector. Pattern Recognition Lett. 23 (11), 1349–1360.

Chen, C.H., Lee, J.S., Sun, Y., 1995. Wavelet transformation for gray-level corner detection. Pattern Recognition 28, 853–861.

Dreschler, L., Nagel, H.H., 1981. Volumetric model and 3D trajectory of a moving car derived from monocular TV frame sequences of a street scene. In: Internat. Joint Conf. on Artificial Intelligence, pp. 692–697.

Fang, J.Q., Huang, T.S., 1982. A corner finding algorithm for image analysis and registration. In: Proc. AAAI Conf., pp. 46–49.

Gao, X.T., Sattar, F., Quddus, A., Venkateswarlu, R., 2007. Multiscale contour corner detection based on local natural scale and wavelet transform. Image Vision Comput. 25 (6), 890–898.

Guru, D.S., Dinesh, R., 2004. Non-parametric adaptive region of support useful for corner detection: A novel approach. Pattern Recognition 37 (1), 165–168.

Harris, C.G., 1987. Determination of ego-motion from matched points. In: Proc. Alvey Vision Conf., Cambridge, UK.

N.H.C. He, X.C. Yung, 2004. Curvature scale space corner detector with adaptive threshold and dynamic region of support. In: IEEE Proc. of the 17th Internat. Conf. on Pattern Recognition, pp. 791–794.

Kitchen, L., Rosenfeld, A., 1982. Gray level corner detection. Pattern Recognition Lett., 95–102.

Lee, J.S., Sun, Y.N., Chen, C.H., 1995. Multiscale Corner detection by using wavelet transform. IEEE Trans. Image Process. 4, 100–104.

Lowe, D., 2004. Distinctive image features from local scale-invariant keypoints. Internat. J. Comput. Vision 2 (60), 91–110.

Masood, A., Sarfraz, M., in press. Corner detection by sliding rectangles along planar curves, Comput. Graph.

Mohanna, F., Mokhtarian, F., 2001. Performance evaluation of corner detection algorithms under similarity and affine transforms. In: Proc. British Machine Vision Conf., pp. 353–362.

Mokhtarian, F., Mackworth, A.K., 1992. A theory of multi-scale, curvature-based shape representation for planar curves. IEEE Trans. Pattern Anal. Machine Intell. 14, 789–805.

Mokhtarian, F., Suomela, R., 1998. Robust image corner detection through curvature scale space. IEEE Trans. Pattern Anal. Machine Intell. 20, 1376–1381.

Mokhtarian, F., Suomela, R., 2001. Enhancing the curvature scale space corner detector. In: Proc. Scandinavian Conf. Image Analysis, pp. 145–152.

Moravec, H.P., 1977. Towards automatic visual obstacle avoidance. In: Proc. Internat. Joint Conf. on Artificial Intelligence, p. 584.

Quddus, A., Gabbouj, M., 2002. Wavelet-based corner detection technique using optimal scale. Pattern Recognition Lett. 23, 215–220.

Rattarangsi, Chin, R.T., 1992. Scale-based detection of corners of planar curves. IEEE Trans. Pattern Anal. Machine Intell. 14, 430–449.

Smith, S.M., Brady, J.M., 1994. SUSAN – A New Approach to Low Level Image Processing, Defence Research Agency, Technical Report No. TR95SMS1, Farnborough, England.

Sobania, A., Paul, J., Evans, O., 2005. Morphological corner detector using paired triangular structuring elements. Pattern Recognition 38 (7), 1087–1098.

Sojka, E., 2002. In: A New and Efficient Algorithm for Detecting the Corners in Digital Images. Lecture Notes in Computer Science, vol. 2449. Springer, Berlin, pp. 125–132.

Tsai, D.M., 1997. Boundary based corner detection using neural networks. Pattern Recognition 30 (1), 85–97.

Tsai, D.M., Hou, H.T., Su, H.J., 1999. Boundary-based corner detection using eigenvalues of covariance matrices. Pattern Recognition Lett. 20, 1–40.

Yeh, C.-H., 2003. Wavelet-based corner detection using eigenvectors of covariance matrices. Pattern Recognition Lett. 24, 2797–2806.

Mohanna, F., Mokhtarian, F., 2001. Performance evaluation of corner detection algorithms under similarity and affine transforms. In: Proc. British Machine Vision Conf., pp. 353–362.